Coalescing binary systems of compact objects to (post)$^{5/2}$-Newtonian order. III. Transition from inspiral to plunge

Lawrence E. Kidder and Clifford M. Will
McDonnell Center for the Space Sciences, Department of Physics, Washington University, St. Louis, Missouri 63130

Alan G. Wiseman
Department of Physics and Astronomy, Northwestern University, Evanston, Illinois 60208
(Received 10 December 1992)

Late in its evolution, a binary system of compact objects will undergo a transition from an adiabatic inspiral induced by gravitational radiation damping to an unstable plunge, induced by strong spacetime curvature. This transition from inspiral to plunge is studied in detail using higher-order post-Newtonian methods. First, we study the innermost stable circular orbits of binary systems of nonrotating, compact objects of arbitrary mass ratio in the absence of gravitational radiation reaction. The method uses "hybrid" two-body equations of motion that are valid through (post)^2-Newtonian order [order $(Gm/rc^2)^2$], but that also include the test-body limit in the Schwarzschild geometry exactly. Using a critical-point analysis, we show that circular orbits inside this innermost orbit are unstable to plunge. The separation of the innermost stable orbit (in harmonic, or de Donder coordinates) is found to vary with mass ratio, from the test-body value of $5m$ to about $6m$ for equal masses, where m is the total mass of the system. The orbital energy, angular momentum, and frequency of the innermost stable orbit are also determined as a function of the ratio of the two masses. We study the sensitivity of these values to higher-order post-Newtonian corrections. Incorporating gravitational radiation reaction in the hybrid equations of motion, we evaluate such variables as radial velocity, angular velocity, energy, and angular momentum for a coalescing binary at the corresponding innermost stable orbit, as a function of mass ratio. These variables could be used as initial conditions for numerical calculations of the ensuing coalescence.

PACS number(s): 04.30.+x, 95.10.Ce, 97.80.Fk

I. INTRODUCTION AND SUMMARY

In two previous papers in this series [1, 2], we have developed a framework for treating the relativistic inspiral of binary systems of compact objects and the gravitational radiation emitted, using higher-order post-Newtonian approximations to general relativity. Inspiraling compact binaries are considered to be the most promising sources of gravitational radiation detectable by laser-interferometric gravitational-wave observatories (for overviews, see [3, 4]). These systems consist of neutron stars or black holes undergoing orbital decay under the dissipative influence of the gravitational radiation reaction, culminating in a final coalescence. Depending on the nature of the system, the final stage could result in (a) transition from steady inspiral to an unstable plunge, leading to either a hydrodynamical coalescence or formation of a black hole, or (b) tidal disruption of any neutron star in the system, leading to a collapsing or accreting disk of matter Each of these scenarios could produce a distinctive signature in the gravitational-wave form in the late-time, high-frequency regime, from which useful information about the system could be extracted [5]. In this paper, we focus on the transition between the steady inspiral and the unstable plunge.

In our earlier work [1], the equations describing the evolution contain all post-Newtonian corrections to the Newtonian two-body equations through (post)$^{5/2}$-Newtonian order, the order at which the dominant gravitational-radiation-reaction damping forces occur. Schematically, these equations can be written

$$d^2\mathbf{x}/dt^2 = -(m\mathbf{x}/r^3)[1 + O(\epsilon) + O(\epsilon^2) + O(\epsilon^{5/2}) + \cdots] , \tag{1.1}$$

where $\mathbf{x}$ and $r = |\mathbf{x}|$ denote the separation vector and distance between the bodies, and $m = m_1 + m_2$ denotes the total mass. We also define the reduced mass $\mu = m_1 m_2/m$. The quantity ϵ denotes the small parameter that characterizes the post-Newtonian expansion, $\epsilon \approx v^2 \approx m/r$, assumed to be smaller than unity ($G = c = 1$).

With the equations of motion, we formally evolved binary-star orbits of arbitrary mass ratio from initial, widely separated orbits that are approximately Keplerian. Gravitational radiation damping causes the orbits both to become more circular if they were initially eccentric, and to spiral inwards, culminating in a final plunge, when the objects coalesce. In practice the evolution must be terminated either when hydrodynamical effects or tidal disruption become important, or when the post-Newtonian approximation ceases to be accurate. We found that, for equal-mass binary orbits evolving from an initial, quasicircular, slow inspiral, there was a transition to a rapid plunge when the separation r was about $6m$. Recall that in the harmonic or de Donder coordinates used in this approach, the event horizon of an isolated black hole is at $r = m$. In the case of a small mass ratio, say, 1:10, gravitational radiation damping is a weaker effect for a given total mass, resulting in a significantly slower inspiral, yet a plunge still occurred around $r = 6m$. On the other hand, an orbital evolution using only the Newtonian equations of motion with the radiation reaction (i.e., without post- or post-post-Newtonian terms) results in a steady inspiral without a plunge, even down to $r \simeq 3m$. These cases are illustrated in Fig. 1.

This suggests the presence of a phenomenon apart from the radiation reaction that is contributing to the transition from a stably inspiraling orbit to an unstable plunge, a phenomenon analogous to the existence of an innermost stable circular orbit (ISCO) for a test particle orbiting a black hole. For Schwarzschild black holes, the radius of the ISCO is $r = 5m$, in harmonic coordinates. For test-body orbits there is no gravitational radiation reaction, and so a circular orbit of radius $r > 5m$ is stable (against small perturbations), whereas an orbit of radius $r < 5m$ is unstable and plunges into the black hole when a perturbation is applied.

This raises the question, is there an analogous ISCO for binary systems whose components have comparable masses? Of course, this cannot be answered rigorously as in the test-body case, because the radiation reaction is necessarily present; nevertheless, we can address the question approximately by the artifice of "shutting off" the radiation-reaction terms in the post-Newtonian equations of motion.

Using the equations of motion described schematically in Eq. (1.1), but keeping only terms through (post)^2-Newtonian order, we find, using a critical-point analysis, that an ISCO does exist at a separation of about $6.8m$, for two equal masses, and at $6.5m$ in the test-body limit. The latter value disagrees with the exact result of $5m$ because of the use of the (post)^2-Newtonian approximation for the test-body equations of motion. Interestingly, when we carry out this method at the first post-Newtonian order, we find that an ISCO does not exist at all (see also Sec. III B).

In order to remedy this inaccuracy in the test-body limit, we adopt a different equation of motion than Eq. (1.1). The terms in Eq. (1.1) turn out to be of two types, those that depend only on the total mass m and those that depend on $\eta = \mu/m$. The former terms can be shown to correspond simply to the (post)^2-Newtonian expansion of the *exact* equations of motion for a test body in a Schwarzschild geometry of total mass m. We *replace* these terms by the exact Schwarzschild expressions. The remaining terms, dependent upon η, we leave as a (post)^2-Newtonian expansion. The resulting hybrid "Schwarzschild–post-Newtonian" equations of motion, which we denote by the subscript H to distinguish them from the standard post-Newtonian equations, are valid to (post)^2-Newtonian order for arbitrary mass ratio [or to (post)$^{5/2}$-Newtonian order if we include the radiation-reaction terms, which are also proportional to η], and are exact in the limit $\eta = \mu/m \to 0$. They are given by

$$(d^2\mathbf{x}/dt^2)_H = -(m/r^2)[A_H\mathbf{n} + B_H\mathbf{v}] , \tag{1.2}$$

where $\mathbf{n} = \mathbf{x}/r$, and where

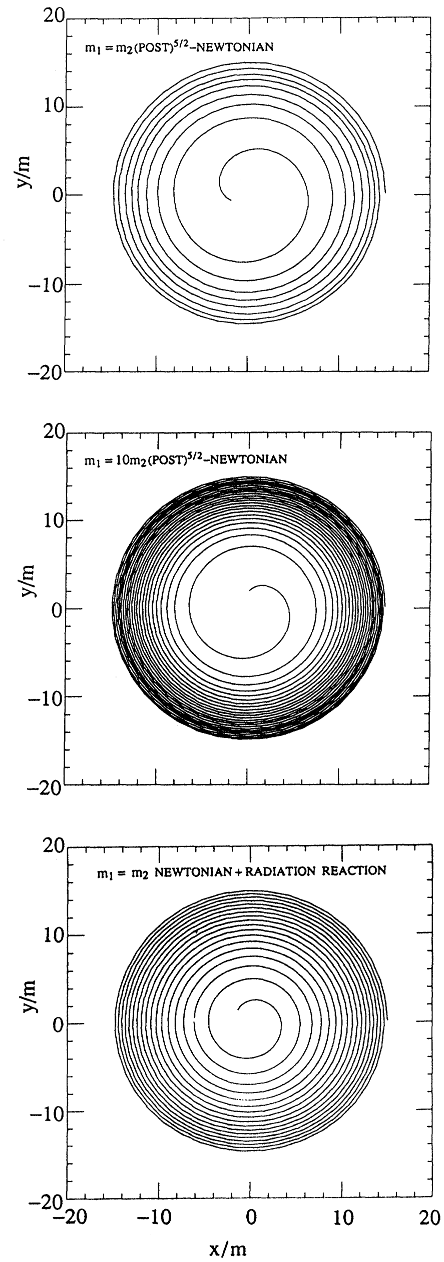

FIG. 1. Inspiral of circular orbits with the gravitational radiation reaction. Top: Equal masses with (post)$^{5/2}$-Newtonian equations of motion; note the transition to a plunge around $r \simeq 6m$. Middle: Mass ratio 10:1; transition to a plunge around $r \simeq 6m$ despite weaker radiation damping. Bottom: Equal masses, Newtonian equations of motion with the radiation reaction; transition to a plunge does not occur.

$$A_H = \left[\frac{1-m/r}{(1+m/r)^3}\right] - \left[\frac{2-m/r}{1-(m/r)^2}\right]\frac{m}{r}\dot{r}^2 + v^2 - \eta\left(2\frac{m}{r} - 3v^2 + \frac{3}{2}\dot{r}^2\right)$$
$$+\eta\left\{\frac{87}{4}\left(\frac{m}{r}\right)^2 + (3-4\eta)v^4 + \frac{15}{8}(1-3\eta)\dot{r}^4 - \frac{3}{2}(3-4\eta)v^2\dot{r}^2 - \frac{1}{2}(13-4\eta)\frac{m}{r}v^2 - (25+2\eta)\frac{m}{r}\dot{r}^2\right\}$$
$$-\frac{8}{5}\eta\frac{m}{r}\dot{r}\left[3v^2 + \frac{17}{3}\frac{m}{r}\right], \tag{1.3a}$$

$$B_H = -\left[\frac{4-2m/r}{1-(m/r)^2}\right]\dot{r} + 2\eta\dot{r} - \frac{1}{2}\eta\dot{r}\left\{(15+4\eta)v^2 - (41+8\eta)\frac{m}{r} - 3(3+2\eta)\dot{r}^2\right\} + \frac{8}{5}\eta\frac{m}{r}\left[v^2 + 3\frac{m}{r}\right]. \tag{1.3b}$$

In Eqs. (1.3), the four sets of terms in each expression denote the Schwarzschild, post-Newtonian, (post)^2-Newtonian, and (post)$^{5/2}$-Newtonian terms, the last three dependent upon η. Note that we no longer have a consistent (post)^2-Newtonian approximation, since we have retained more "terms," or accuracy in powers of m/r, in the Schwarzschild sector than we have in the η sector, but we believe that obtaining the correct test-mass limit outweighs this concern. We discuss the accuracy of this approach later (Sec. III D).

We then use a critical-point analysis to find the ISCO of the H equations [6]. We first drop the final, radiation-reaction terms from A_H and B_H. Choosing the fixed orbital plane to be equatorial, we convert the H equations of motion into a radial and an angular equation. Circular orbits correspond to critical points $\dot{r} = \ddot{r} = \dot{\omega} = 0$, where ω is the angular frequency. We linearize about the critical point, and determine the innermost stable orbit as that value of r_0 for which the perturbation changes from oscillatory to exponential in time. In this procedure the relevant expressions for A_H and B_H are treated as exact, and the values of r_0 determined numerically.

The result as a function of the parameter η is plotted in Fig. 2 [7]. Note that η is related to the mass ratio by $\eta = X/(1+X)^2$, where $X = m_1/m_2$; $\eta = 0.25$ corresponds to equal masses. The separation increases from the exact Schwarzschild value of $5m$ at $\eta = 0$ to about $6.03m$ for equal masses, and is roughly linear in η. We also checked these results using a direct numerical integration of the H equations of motion (without the radiation reaction) for perturbed circular orbits to search for unstable points. It is interesting to note that, for two $1.4M_\odot$ neutron stars, the ISCO radius corresponds to a coordinate separation of about 25 km, which is larger than the sum of the two neutron-star radii for all but the stiffest equations of state.

The variable r is not a directly measurable or gauge-invariant quantity, and so its utility is limited. However, the binding energy per reduced mass $\tilde{E}$ (total energy minus rest-mass energies of the binary components, divided by reduced mass), and angular momentum per

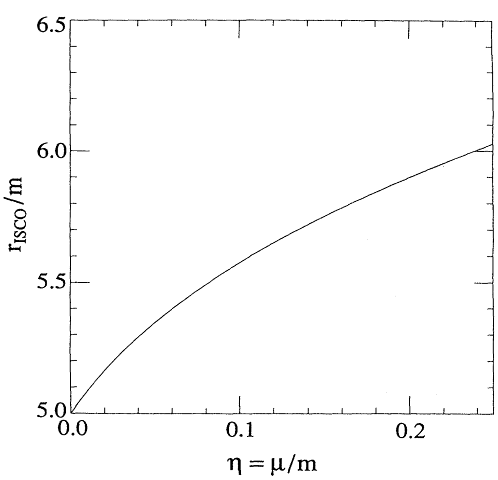

FIG. 2. Harmonic coordinate separation of the innermost stable circular orbit as a function of $\eta = \mu/m$.

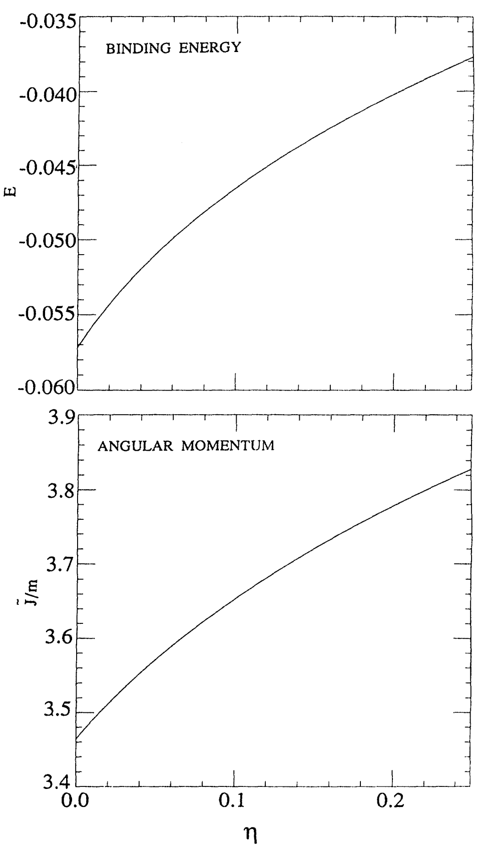

FIG. 3. Energy per reduced mass and angular momentum per reduced mass at the ISCO as functions of η.

reduced mass $\tilde{J}$ are invariant quantities. By analogy with the equations of motion, we have developed hybrid (post)^2-Newtonian expressions for $\tilde{E}$ and $\tilde{J}$ that reproduce the Schwarzschild test-body results and that are valid to (post)^2-Newtonian order for an arbitrary mass ratio. In the test-body limit, they correspond to the exact Schwarzschild expressions, written in harmonic coordinates. Through (post)^2-Newtonian order, they agree with standard results obtainable from Lagrangian formulations of the equations of motion [8]. The results are plotted in Fig. 3. We also obtain the orbital frequency of the ISCO measured asymptotically, $f = \omega_0/2\pi$, directly from the critical-point analysis. The result is plotted in Fig. 4. The gravitational-wave frequency is twice the orbital frequency.

Using the hybrid equations of motion including the gravitational radiation reaction, we evolve inspiraling orbits for various mass ratios up to the corresponding ISCO radius, which we regard as the transition point between inspiral and plunge. At this radius, we evaluate the radial and azimuthal velocities, the orbital frequency, and the energy and angular momentum of the inspiraling orbit. The results for v_r as a function of η are plotted in Fig. 5, with corresponding values for v_ϕ at $\eta = 0$ and $\eta = 1/4$ labeled. Values of the relevant orbital quantities in the equal-mass case are listed in Table I. Because v_r is at most 10 times smaller than v_ϕ, it is adequate to use the circular orbit results for energy, angular momentum, and orbital frequency in the inspiral case, since v_r affects these quantities only quadratically. Note that, for equal masses at the ISCO, $E = -0.94 \times 10^{-2} m$, so that a little less than 1% of the total mass of the system has been radiated away in gravitational waves. When properly converted to the appropriate coordinates, these values may provide useful initial conditions for large-scale numerical simulations of the plunge and coalescence process.

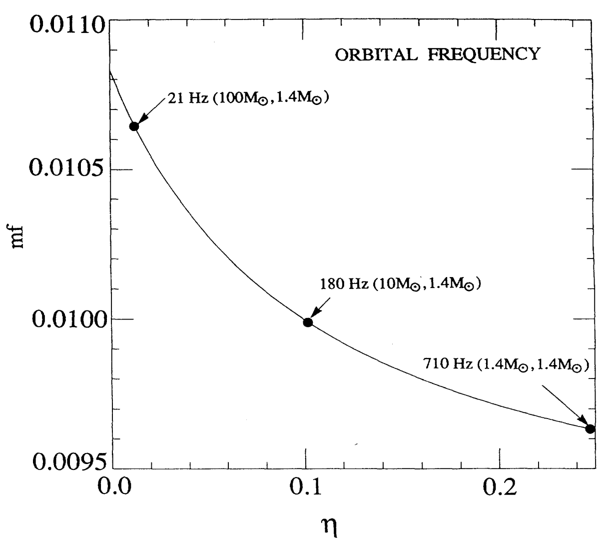

FIG. 4. Orbital frequency of the ISCO as seen asymptotically, as a function of η. Specific values of frequency in Hz are shown for various masses. Gravitational-wave frequency is double the orbital frequency.

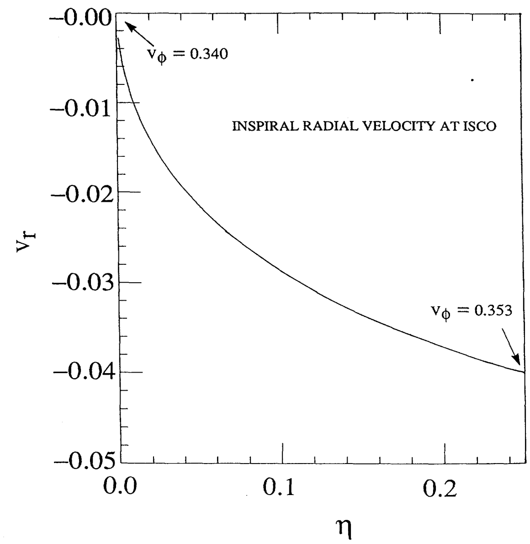

FIG. 5. Radial velocity v_r at the ISCO for inspiral orbits, as a function of η. Azimuthal velocity v_ϕ for the corresponding orbits is labeled for $\eta = 0$ and $1/4$.

The remainder of this paper presents details. In Sec. II we develop the hybrid equations of motion and derive the corresponding hybrid expressions for energy and angular momentum. In Sec. III we use a critical-point analysis to determine the coordinate separation of the ISCO, and discuss the accuracy of the estimate by considering the influence of (post)^3-Newtonian effects. In Sec. IV we study orbital evolution using the hybrid equations of motion including the radiation reaction to determine the actual state of the orbit at the ISCO radius. In Sec. V we compare our results with other work, discuss the relevance of these results to observation of gravitational radiation using laser-interferometric gravitational-wave observatories, and make concluding remarks.

II. HYBRID EQUATIONS OF MOTION FOR BINARY SYSTEMS

A. Equations of motion

We begin with the equations of motion for two bodies of arbitrary mass developed by Damour and Deruelle [9]. These equations contain all post-Newtonian corrections through (post)$^{5/2}$-Newtonian order, including effects due to the radiation reaction. They also contain

TABLE I. Orbital variables at the ISCO of inspiraling equal-mass binary system.

Orbital variable	Value
v_r	-3.99×10^{-2}
v_ϕ	0.353
mf	9.33×10^{-3}
$\tilde{E}$	-3.69×10^{-2}
$\tilde{J}/m$	3.95

terms depending upon the spins of the bodies, but we will defer consideration of spin effects to future publications. The Damour-Deruelle equations do not include tidal effects; for binary systems containing neutron stars or black holes, these are expected to have little effect on the instantaneous orbit until the very latest stage of inspiral and coalescence, although they could affect the long-term accumulations of orbital phase [12].

Using an integral of the motion which can be taken as the center of mass of the system, Lincoln and Will [1] converted the two-body equations of motion to an effective one-body equation of motion. The relative acceleration is then given by

$$\mathbf{a} \equiv \mathbf{a}_1 - \mathbf{a}_2 = -(m/r^2)[A\mathbf{n} + B\mathbf{v}] , \tag{2.1}$$

where $A \equiv 1 + A_1 + A_2 + A_{5/2}$, $B \equiv B_1 + B_2 + B_{5/2}$, the subscript indicates the order of the post-Newtonian correction terms in terms of powers of the small parameter $\epsilon = m/r = v^2$, and

$$A_1 = -2(2+\eta)\frac{m}{r} + (1+3\eta)v^2 - \frac{3}{2}\eta\dot{r}^2 , \tag{2.2a}$$

$$\begin{aligned} A_2 = {} & \frac{3}{4}(12+29\eta)\left(\frac{m}{r}\right)^2 + \eta(3-4\eta)v^4 + \frac{15}{8}\eta(1-3\eta)\dot{r}^4 \\ & -\frac{3}{2}\eta(3-4\eta)v^2\dot{r}^2 - \frac{1}{2}\eta(13-4\eta)\frac{m}{r}v^2 \\ & -(2+25\eta+2\eta^2)\frac{m}{r}\dot{r}^2 , \end{aligned} \tag{2.2b}$$

$$A_{5/2} = -\frac{8}{5}\eta\frac{m}{r}\dot{r}\left[3v^2 + \frac{17}{3}\frac{m}{r}\right] , \tag{2.2c}$$

$$B_1 = -2(2-\eta)\dot{r} , \tag{2.2d}$$

$$\begin{aligned} B_2 = -\frac{1}{2}\dot{r}\Bigg[& \eta(15+4\eta)v^2 - (4+41\eta+8\eta^2)\frac{m}{r} \\ & -3\eta(3+2\eta)\dot{r}^2\Bigg] , \end{aligned} \tag{2.2e}$$

$$B_{5/2} = \frac{8}{5}\eta\frac{m}{r}\left[v^2 + 3\frac{m}{r}\right] , \tag{2.2f}$$

where an overdot denotes d/dt.

Note that the terms in A and B can be separated into two types, those that depend only on the total mass m and those that depend upon the reduced mass $\mu = \eta m$. In the test-mass (TM) limit ($\mu \to 0$) A and B reduce to

$$A_{\rm TM} = 1 - 4\frac{m}{r} + v^2 + 9\left(\frac{m}{r}\right)^2 - 2\frac{m}{r}\dot{r}^2 , \tag{2.3a}$$

$$B_{\rm TM} = -\dot{r}(4 - 2m/r) . \tag{2.3b}$$

We will now show that $A_{\rm TM}$ and $B_{\rm TM}$ correspond to the (post)^2-Newtonian expansion of the exact equations of motion for a test body in a Schwarzschild geometry of total mass m.

In harmonic coordinates, the coordinates in which the Damour-Deruelle equations were obtained, the Schwarzschild metric is given by

$$\begin{aligned} ds^2 = {} & -\left[\frac{r-m}{r+m}\right]dt^2 + \left[\frac{r+m}{r-m}\right]dr^2 \\ & +(r+m)^2(d\theta^2 + \sin^2\theta d\phi^2) . \end{aligned} \tag{2.4}$$

Harmonic coordinates are related to the usual Schwarzschild coordinates by the transformation $r_s \longrightarrow r_h + m$. Using the geodesic equation, we obtain the following relative acceleration:

$$\mathbf{a}_S = -(m/r^2)[A_S\mathbf{n} + B_S\mathbf{v}] , \tag{2.5}$$

where

$$A_S = \left[\frac{1-m/r}{(1+m/r)^3}\right] - \left[\frac{2-m/r}{1-(m/r)^2}\right]\frac{m}{r}\dot{r}^2 + v^2 , \tag{2.6a}$$

$$B_S = -\left[\frac{4-2m/r}{1-(m/r)^2}\right]\dot{r} . \tag{2.6b}$$

Expanding A_S and B_S in powers of ϵ gives

$$A_S = 1 - 4\frac{m}{r} + v^2 + 9\left(\frac{m}{r}\right)^2 - 2\frac{m}{r}\dot{r}^2 + O(\epsilon^3) , \tag{2.7a}$$

$$B_S = -4\dot{r} + 2\frac{m}{r}\dot{r} + O(\epsilon^3) . \tag{2.7b}$$

Therefore we see that $A_{\rm TM}$ and $B_{\rm TM}$ correspond simply to the (post)^2-Newtonian expansion of A_S and B_S.

We obtain a second set of equations of motion by replacing the test-mass terms $A_{\rm TM}$ and $B_{\rm TM}$ in Eqs. (2.2) with the exact Schwarzschild terms A_S and B_S. The resulting "hybrid" (H) equations of motion are given by Eqs. (1.2) and (1.3). They are valid through (post)$^{5/2}$-Newtonian order for arbitrary masses, and are exact in the test-mass limit.

B. Constants of the motion

The Damour-Deruelle two-body equations of motion through (post)^2-Newtonian order can be derived from a generalized Lagrangian [8], that is, a Lagrangian which is a function of the positions, velocities, and accelerations of the two bodies. Likewise the relative equations of motion [Eqs. (2.1) and (2.2)] can be derived from a generalized Lagrangian which is a function of the relative position, velocity, and acceleration of the system. This Lagrangian can be obtained from the two-body Lagrangian (Eqs. (164)–(169) of [9]) by using the transformations

$$\begin{aligned} v_1^i = {} & v^i\left[\frac{m_2}{m} + \frac{1}{2}\eta\frac{\delta m}{m}\left(v^2 - \frac{m}{r}\right)\right] \\ & +n^i\eta\frac{\delta m}{m}\left[r(\mathbf{v}\cdot\mathbf{a}) + \frac{1}{2}\frac{m}{r}(\mathbf{n}\cdot\mathbf{v})\right] , \end{aligned} \tag{2.8a}$$

$$\begin{aligned} v_2^i = {} & v^i\left[-\frac{m_1}{m} + \frac{1}{2}\eta\frac{\delta m}{m}\left(v^2 - \frac{m}{r}\right)\right] \\ & +n^i\eta\frac{\delta m}{m}\left[r(\mathbf{v}\cdot\mathbf{a}) + \frac{1}{2}\frac{m}{r}(\mathbf{n}\cdot\mathbf{v})\right] , \end{aligned} \tag{2.8b}$$

$$a_1^i = a^i\left[\frac{m_2}{m} + O(\epsilon)\right] , \tag{2.8c}$$

$$a_2^i = -a^i\left[\frac{m_1}{m} + O(\epsilon)\right] . \tag{2.8d}$$

These are obtained from an integral of the motion of the two-body Lagrangian which can be taken as the center of mass [10]. Using the transformations (2.8) on the two-body Lagrangian of [9], we find that the Lagrangian for the relative system is given by

$$\begin{aligned} L = \mu\Big\{ & \frac{1}{2}v^2 + \frac{m}{r} + \frac{1}{8}(1-3\eta)v^4 + \frac{1}{2}(3+\eta)\frac{m}{r}v^2 + \frac{1}{2}\eta\frac{m}{r}(\mathbf{n}\cdot\mathbf{v})^2 - \frac{1}{2}\left(\frac{m}{r}\right)^2 \\ & + \frac{1}{16}(1-7\eta+13\eta^2)v^6 + \frac{1}{8}(7-10\eta-9\eta^2)v^4\frac{m}{r} + \frac{1}{4}\eta(1-5\eta)v^2\frac{m}{r}(\mathbf{n}\cdot\mathbf{v})^2 \\ & + \frac{3}{8}\eta^2\frac{m}{r}(\mathbf{n}\cdot\mathbf{v})^4 + \frac{1}{8}(14-27\eta+4\eta^2)v^2\left(\frac{m}{r}\right)^2 + \frac{1}{8}(4+45\eta-4\eta^2)\left(\frac{m}{r}\right)^2(\mathbf{n}\cdot\mathbf{v})^2 \\ & + \frac{1}{4}(2+15\eta)\left(\frac{m}{r}\right)^3 + \frac{1}{2}\eta(1-4\eta)r^2(\mathbf{v}\cdot\mathbf{a})^2 + \frac{7}{8}\eta v^2\frac{m}{r}r(\mathbf{n}\cdot\mathbf{a}) \\ & - \frac{1}{8}\eta\frac{m}{r}(\mathbf{n}\cdot\mathbf{v})^2 r(\mathbf{n}\cdot\mathbf{a}) - \frac{1}{4}\eta(3+16\eta)\frac{m}{r}(\mathbf{n}\cdot\mathbf{v})r(\mathbf{v}\cdot\mathbf{a})\Big\} . \end{aligned} \tag{2.9}$$

Defining the quantities

$$p^i \equiv \frac{\partial L}{\partial v^i} - \frac{d}{dt}\left(\frac{\partial L}{\partial a^i}\right) , \; s^i \equiv \frac{\partial L}{\partial a^i} , \tag{2.10}$$

it is fairly straightforward to show that the relative equations of motion through (post)^2-Newtonian order, Eqs. (2.1) and (2.2), are given by the Euler-Lagrange equations

$$\partial L/\partial x^i - dp^i/dt = 0 , \tag{2.11}$$

where it is understood that wherever the acceleration appears in a higher-order term in Eq. (2.11), one substitutes the lower-order equation of motion.

The relative Lagrangian is invariant with respect to time translations and spatial rotations so that there exist constants of the motion, namely, the energy and angular momentum, given by

$$E = (\mathbf{p}\cdot\mathbf{v}) + (\mathbf{s}\cdot\mathbf{a}) - L , \tag{2.12a}$$

$$\mathbf{J} = \mathbf{x}\times\mathbf{p} + \mathbf{v}\times\mathbf{s}. \tag{2.12b}$$

Evaluating these expressions and replacing the relative acceleration by the appropriate lower-order expression from the equations of motion, we obtain

$$\begin{aligned} E = \mu\Big\{ & \frac{1}{2}v^2 - \frac{m}{r} + \frac{3}{8}(1-3\eta)v^4 + \frac{1}{2}(3+\eta)v^2\frac{m}{r} + \frac{1}{2}\eta\frac{m}{r}\dot{r}^2 + \frac{1}{2}\left(\frac{m}{r}\right)^2 \\ & + \frac{5}{16}(1-7\eta+13\eta^2)v^6 + \frac{1}{8}(21-23\eta-27\eta^2)\frac{m}{r}v^4 + \frac{1}{4}\eta(1-15\eta)\frac{m}{r}v^2\dot{r}^2 \\ & - \frac{3}{8}\eta(1-3\eta)\frac{m}{r}\dot{r}^4 + \frac{1}{8}(14-55\eta+4\eta^2)\left(\frac{m}{r}\right)^2 v^2 + \frac{1}{8}(4+69\eta+12\eta^2)\left(\frac{m}{r}\right)^2\dot{r}^2 - \frac{1}{4}(2+15\eta)\left(\frac{m}{r}\right)^3\Big\} , \end{aligned} \tag{2.13a}$$

$$\begin{aligned} \mathbf{J} = \mu(\mathbf{r}\times\mathbf{v})\Big\{ & 1 + \frac{1}{2}v^2(1-3\eta) + (3+\eta)\frac{m}{r} + \frac{3}{8}(1-7\eta+13\eta^2)v^4 \\ & + \frac{1}{2}(7-10\eta-9\eta^2)\frac{m}{r}v^2 - \frac{1}{2}\eta(2+5\eta)\frac{m}{r}\dot{r}^2 + \frac{1}{4}(14-41\eta+4\eta^2)\left(\frac{m}{r}\right)^2\Big\} . \end{aligned} \tag{2.13b}$$

These are (post)^2-Newtonian constants of the motion; radiation damping is being ignored.

As we did with the equations of motion, we can separate the energy and angular momentum into terms which depend only upon the total mass m and those that depend upon the reduced mass μ, apart from the overall multiplicative factor of μ. In the test-mass limit we have, for the "reduced" energy and angular momentum $\tilde{E}_{\rm TM}$ and $\tilde{\mathbf{J}}_{\rm TM}$,

$$\begin{aligned} \tilde{E}_{\rm TM} \equiv E_{\rm TM}/\mu = & \frac{1}{2}v^2 - \frac{m}{r} + \frac{3}{8}v^4 + \frac{3}{2}\frac{m}{r}v^2 + \frac{1}{2}\left(\frac{m}{r}\right)^2 \\ & + \frac{5}{16}v^6 + \frac{21}{8}v^4\frac{m}{r} + \frac{7}{4}v^2\left(\frac{m}{r}\right)^2 \\ & + \frac{1}{2}\dot{r}^2\left(\frac{m}{r}\right)^2 - \frac{1}{2}\left(\frac{m}{r}\right)^3 , \end{aligned} \tag{2.14a}$$

$$\tilde{\mathbf{J}}_{\rm TM} \equiv \mathbf{J}_{\rm TM}/\mu = (\mathbf{r}\times\mathbf{v})\left[1+\frac{1}{2}v^2+3\frac{m}{r}+\frac{7}{2}\frac{m}{r}v^2 +\frac{3}{8}v^4+\frac{7}{2}\left(\frac{m}{r}\right)^2\right]. \tag{2.14b}$$

We will now show that $\tilde{E}_{\rm TM}$ and $\tilde{\mathbf{J}}_{\rm TM}$ are just the (post)^2-Newtonian expansions of the Schwarzschild reduced energy and angular momentum. For a geodesic, these quantities are given by $\tilde{E} = -g_{00}u^0$, $\tilde{J} = g_{\phi\phi}u^\phi$, where u^α are components of the four-velocity, so that, in harmonic coordinates,

$$\tilde{E} = \frac{dt}{d\tau}\left(\frac{r-m}{r+m}\right), \quad \tilde{J} = \frac{d\phi}{d\tau}(r+m)^2, \tag{2.15}$$

where we have restricted motion to the plane $\theta = \frac{\pi}{2}$ without loss of generality. We also have the energy equation from $u^\alpha u_\alpha = -1$,

$$\tilde{E}^2 = \left(\frac{dr}{d\tau}\right)^2 + \frac{r-m}{r+m}\left[1+\frac{\tilde{J}^2}{(r+m)^2}\right]. \tag{2.16}$$

Combining Eqs. (2.15) and (2.16) to solve for $dt/d\tau$, substituting that into the first of Eqs. (2.15), and subtracting the unit rest-mass contribution from $\tilde{E}$, we obtain the Schwarzschild "binding" energy and angular momentum

$$\tilde{E}_S = \left(\frac{r-m}{r+m}\right)^{1/2}\left[1-v^2\frac{(r+m)^3}{r^2(r-m)} -\dot{r}^2\left(\frac{r+m}{r-m}\right)^2\left(\frac{m}{r}\right)^2\right]^{-1/2} - 1, \tag{2.17a}$$

$$\tilde{J}_S = \dot{\phi}\left[\frac{(r+m)^5}{r-m}\right]^{1/2}\left[1-v^2\frac{(r+m)^3}{r^2(r-m)} -\dot{r}^2\left(\frac{r+m}{r-m}\right)^2\left(\frac{m}{r}\right)^2\right]^{-1/2}. \tag{2.17b}$$

It is straightforward to expand these quantities in terms of ϵ and obtain precisely Eqs. (2.14a) and (2.14b) through $O(\epsilon^2)$. We see that the test-mass terms of the (post)^2-Newtonian energy and angular momentum are just the (post)^2-Newtonian expansion of the Schwarzschild energy and angular momentum. We therefore *replace* $\tilde{E}_{\rm TM}$ by $\tilde{E}_S$ and $\tilde{J}_{\rm TM}$ by $\tilde{J}_S$, and obtain the following hybrid constants of the motion:

$$\begin{aligned}\tilde{E}_H = {} & \left(\frac{r-m}{r+m}\right)^{1/2}\left[1-v^2\frac{(r+m)^3}{r^2(r-m)}-\dot{r}^2\left(\frac{r+m}{r-m}\right)^2\left(\frac{m}{r}\right)^2\right]^{-1/2} - 1 - \eta\left(\frac{9}{8}v^4-\frac{1}{2}v^2\frac{m}{r}-\frac{1}{2}\frac{m}{r}\dot{r}^2\right)\\ & -\eta\left\{\frac{5}{16}(7-13\eta)v^6+\frac{1}{8}(23+27\eta)\frac{m}{r}v^4-\frac{1}{4}(1-15\eta)\frac{m}{r}v^2\dot{r}^2\right.\\ & \left.+\frac{3}{8}(1-3\eta)\frac{m}{r}\dot{r}^4+\frac{1}{8}(55-4\eta)\left(\frac{m}{r}\right)^2v^2-\frac{3}{8}(23+4\eta)\left(\frac{m}{r}\right)^2\dot{r}^2+\frac{15}{4}\left(\frac{m}{r}\right)^3\right\},\end{aligned} \tag{2.18a}$$

$$\begin{aligned}\tilde{J}_H = r^2\dot{\phi}\Bigg(& \left[\frac{(r+m)^5}{r^4(r-m)}\right]^{1/2}\left[1-v^2\frac{(r+m)^3}{r^2(r-m)}-\dot{r}^2\left(\frac{r+m}{r-m}\right)^2\left(\frac{m}{r}\right)^2\right]^{-1/2} - \eta\left(\frac{3}{2}v^2-\frac{m}{r}\right)\\ & -\eta\left\{\frac{3}{8}(7-13\eta)v^4+\frac{1}{2}(10+9\eta)\frac{m}{r}v^2+\frac{1}{2}(2+5\eta)\frac{m}{r}\dot{r}^2+\frac{1}{4}(41-4\eta)\left(\frac{m}{r}\right)^2\right\}\Bigg).\end{aligned} \tag{2.18b}$$

The first group of terms in each expression corresponds to the exact Schwarzschild test-body ($\eta = 0$) values, the second group to post-Newtonian, finite-mass terms, and the remaining terms to (post)^2-Newtonian finite-mass terms. These expressions will be used henceforth to evaluate the energy and momentum of orbits evolved using the hybrid equations of motion.

III. CRITICAL-POINT ANALYSIS OF THE INNERMOST CIRCULAR ORBIT

A. General condition for stable circular orbits

In order to study the existence of an innermost stable circular orbit, we drop the gravitational-radiation-reaction terms from the equations of motion. We first consider general equations of motion of the form of Eq. (2.1) without reaction terms. Later we will specialize to the (post)^2-Newtonian, Schwarzschild, and hybrid equations of motion. Orienting the coordinate system so that the orbit is in the x-y plane, we separate the equation into radial and angular equations

$$\ddot{r} = -(m/r^2)(A+B\dot{r}) + r\dot{\phi}^2, \tag{3.1a}$$

$$\ddot{\phi} = -\dot{\phi}[(m/r^2)B + 2\dot{r}/r]. \tag{3.1b}$$

Defining $\omega \equiv \dot{\phi}$ and $u \equiv \dot{r}$, we have the system of equations

$$\dot{r} = u, \tag{3.2a}$$

$$\dot{u} = -(m/r^2)(A+Bu) + r\omega^2, \tag{3.2b}$$

$$\dot{\omega} = -\omega[(m/r^2)B + 2u/r], \tag{3.2c}$$

where we note that $v^2 = u^2 + r^2\omega^2$. A circular orbit is a critical point of this system where $\dot{r} = \dot{u} = \dot{\omega} = 0$, which implies $u = 0$. We also note that for all cases considered here, B is proportional to $\dot{r}$; thus, $B = 0$ at the critical point [11]. Equation (3.2b) then yields the circular orbit condition

$$\omega_0^2 = mA_0/r_0^3\,, \tag{3.3}$$

from which we can obtain ω_0 as a function of r_0. Perturbing about the critical values r_0, ω_0, and $u_0 = 0$ by variables ϵ_r, ϵ_ω, and ϵ_u, respectively, and working to linear order in ϵ_i, it is straightforward to obtain the system of equations

$$\dot{\epsilon}_r = \epsilon_u\,,\quad \dot{\epsilon}_u = a\epsilon_r + b\epsilon_\omega\,,\quad \dot{\epsilon}_\omega = c\epsilon_u\,, \tag{3.4}$$

where

$$a = 3\omega_0^2 - (m/r_0^2)(\partial A/\partial r)_0\,, \tag{3.5a}$$

$$b = 2r_0\omega_0 - (m/r_0^2)(\partial A/\partial \omega)_0\,, \tag{3.5b}$$

$$c = -\omega_0\left[2/r_0 + (m/r_0^2)(\partial B/\partial u)_0\right]\,. \tag{3.5c}$$

We have used the fact that, for all cases considered, A depends quadratically on u, so that $\partial A/\partial u \propto u$ [11]. With the ansatz $\epsilon_i = E_i e^{i\lambda t}$, we obtain the eigenvalue conditions $\lambda = 0$ and $\lambda = \pm(-a-bc)^{1/2}$. The first eigenvalue corresponds to a solution with $\epsilon_u = 0$ and $\epsilon_\omega = -(a/b)\epsilon_r$, which is a displacement from one circular orbit to a neighboring circular orbit. The other eigenvalues correspond to evolving orbits; for stable, oscillatory solutions, we must have $a + bc < 0$, which translates into the condition

$$1 - 2\frac{\omega_0}{A_0}\left(\frac{\partial A}{\partial \omega}\right)_0 + \frac{r_0}{A_0}\left(\frac{\partial A}{\partial r}\right)_0 + 2\frac{m}{r_0}\left(\frac{\partial B}{\partial u}\right)_0\left[1 - \frac{1}{2}\frac{\omega_0}{A_0}\left(\frac{\partial A}{\partial \omega}\right)_0\right] > 0\,. \tag{3.6}$$

This, together with Eq. (3.3), gives an equation for r_0 for stable circular orbits. An innermost stable circular orbit corresponds to a minimum r_0 that satisfies Eq. (3.6).

B. Innermost stable orbits for Schwarzschild geometry

For test-body motion in Schwarzschild geometry, we use A_S and B_S from Eqs. (2.6), substitute $\dot{r} = u$ and $v^2 = u^2 + r^2\omega^2$, and calculate the appropriate partial derivatives. The circular orbit condition is then ${\omega_0}^2 = m/(r_0+m)^3$, and the stability condition Eq. (3.6) becomes $(1 - 5m/r_0)/(1 + m/r_0) > 0$, which yields the well-known innermost stable orbit at $r_0 = 5m$.

One can also calculate the innermost stable orbit at each order of approximation to the Schwarzschild geometry, post-Newtonian, (post)^2-Newtonian, and so on by simply expanding the functions A_S and B_S in powers of m/r and truncating at the appropriate order, and then repeating the above procedure. Because there is no radiation reaction for test-body motion, this procedure can be carried out to indefinitely high order in principle. The resulting radii are shown in Table II. At post- and (post)^3-Newtonian order, the solutions correspond to spurious roots that do not converge to $5m$. Note that the convergent solutions only approach $5m$ at (post)^6-Newtonian order. This suggests that motion in the Schwarzschild geometry is not a rapidly converging series in a post-Newtonian expansion. This behavior has also been seen in the problem of gravitational radiation from test-body motion in Schwarzschild geometry [5]. This is in part what motivates our use of the hybrid equations of motion, to get the Schwarzschild behavior exactly.

TABLE II. Test-body ISCO radii for (post)^n-Newtonian expansion of Schwarzschild equations of motion.

Post-Newtonian order (n)	$r_{\rm ISCO}/m$
1	a
2	6.505
3	a
4	5.364
5	4.784
6	5.048
7	4.985
8	5.004
9	4.999
10	5.000

[a]Spurious root of equations for critical point.

C. Innermost stable orbits for hybrid equations of motion

Taking now the hybrid equations of motion, Eqs. (1.2) and (1.3), substituting $u = \dot{r}$ and $v^2 = u^2 + r^2\omega^2$, and taking the appropriate partial derivatives of A_H and B_H, we substitute the results into Eqs. (3.3) and (3.6). These are coupled, algebraic equations in ${\omega_0}^2$ and r_0, which we solve, treating them as exact. The equations are equivalent to a polynomial equation for r_0 of high degree; in order to select the appropriate root, we first solve in the test mass ($\eta = 0$) limit and then follow that root as η increases. The resulting values of r_0 are plotted in Fig. 2. These, together with the resulting value of ω_0, are then substituted into Eqs. (2.18a) and (2.18b) to yield Fig. 3. Figure 4 plots $mf = 2m\pi\omega_0$ for the innermost orbit as a function of η.

D. Accuracy: Effects of (post)^3-Newtonian terms

Because the separation radius of the innermost orbit for equal masses corresponds to $m/r_0 = 1/6$, which is not all that small, one might question the accuracy of our estimate. Indeed, if one repeats the analysis of the previous subsection using the fully (post)^2-Newtonian equations of motion, Eqs. (2.1) and (2.2), the results are $r_0 \approx 6.51m$ for the test-body limit and $r_0 \approx 6.8m$ for the equal-mass case, the former value coinciding, as expected, with the (post)^2-Newtonian Schwarzschild value of Table I. However, we conjecture that this discrepancy is dominated by the Schwarzschild behavior, which is poorly convergent.

Our hybrid equation of motion is an attempt to cure this defect.

One might still ask how accurately we have determined the variation of the innermost orbit with η. Indeed, if we determine the innermost orbit using the hybrid equations together with only the first post-Newtonian, non-test-mass terms, we find that r_0 *decreases* from $5m$ in the test-mass limit to about $3.5m$ at $\eta \approx 0.13$, whereupon no further solutions exist. Including the (post)^2-Newtonian non-test-mass terms leads to the solutions increasing from $5m$ to $6.03m$ plotted in Fig. 2. Given the large change between the post- and (post)^2-Newtonian approximations, we must address the accuracy of this result. We have done so by looking at the effects of (post)^3-Newtonian, non-test-mass terms on the estimate of r_0 (we already have the test-mass terms exactly in the hybrid equations). Unfortunately, such terms have not been derived to date. Nevertheless, we can analyze the effects of a range of possibilities. At (post)^3-Newtonian order, the terms in the hybrid equations of motion should have the general form

$$\delta \mathbf{a} = -\eta(m/r^2)[A_3\mathbf{n} + B_3\mathbf{v}] \,, \tag{3.7}$$

where we have factored out an overall η, as in Eqs. (1.3). The term A_3 will generally consist of a linear combination of all terms of order ϵ^3, such as v^6, $(m/r)^3$, $v^4\dot{r}^2$, and so on, a total of ten terms. Similarly, B_3 will consist of $\dot{r}$ times a linear combination of terms of order ϵ^2, such as v^4, v^2m/r, and so on, for a total of six terms. However, because our critical-point analysis involves a first-order perturbation about an orbit with $\dot{r} = 0$, we can ignore any terms of quadratic or higher order in $\dot{r}$. This leaves seven possible terms, and so we write

$$A_3 = \alpha_0 v^6 + \alpha_1 v^4\left(\frac{m}{r}\right) + \alpha_2 v^2\left(\frac{m}{r}\right)^2 + \alpha_3\left(\frac{m}{r}\right)^3 , \tag{3.8a}$$

$$B_3 = \dot{r}\left[\beta_0 v^4 + \beta_1 v^2\left(\frac{m}{r}\right) + \beta_3\left(\frac{m}{r}\right)^2\right] . \tag{3.8b}$$

We now repeat the calculation of the innermost orbit for the special case of equal masses ($\eta = 1/4$). We consider the seven cases in which all but one parameter are zero, while that parameter varies between $+10$ and -10. The results are plotted in Fig. 6. We note that the maximum variation from our value of $r_0 \approx 6.03$ is only about 5% over the range considered. For $\eta < 1/4$, the percentage variations will be even smaller because of the overall η dependence in Eq. (3.7).

IV. ORBIT EVOLUTION FROM INSPIRAL TO PLUNGE

The foregoing results establish the location of an innermost stable circular orbit for a binary system of arbitrary mass ratio, in the absence of the gravitational radiation reaction. Of course, except in the test-mass limit, the gravitational radiation reaction is necessarily present. We now use the full hybrid equations of motion to evolve coalescing orbits with the radiation reaction down to the corresponding innermost circular orbit. These evolutions begin from a quasicircular orbit at a starting separation of $15m$, and are evolved numerically by direct integration of the hybrid equations of motion. A potentially useful product of such a calculation is a set of values of the orbital parameters, such as $v_r \equiv \dot{r}$, ω, $v_\phi \equiv r\omega$, $\tilde{E}$, and $\tilde{J}$ that a realistic coalescing system might be expected to possess. The radial velocity v_r is plotted as a function of η in Fig. 5. Because $v_r << 1$, the other quantities can be estimated to sufficient accuracy using the circular, noninspiraling orbits at the ISCO.

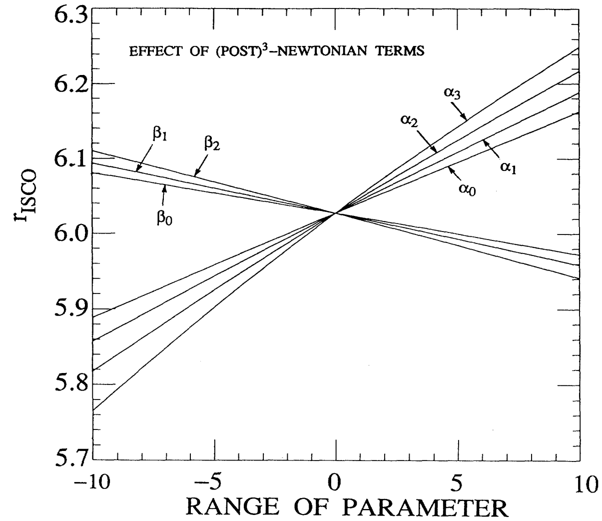

FIG. 6. Effect of (post)^3-Newtonian terms on the separation of the ISCO. Effect of varying each parameter in Eqs. (3.8) in turn between -10 and $+10$ is shown. Maximum variation is about 5%.

After the system reaches the innermost circular orbit, it undergoes a rapid plunge, and it is very likely that fully three-dimensional general relativistic computer codes (with or without hydrodynamics, depending on whether neutron stars are present) will take over the analysis of the evolution. When properly converted into the variables appropriate for numerical relativity, the results shown in Fig. 5 could provide initial conditions for such codes (see [13] for a review). This interface with numerical relativity is currently under study.

V. DISCUSSION

The first detailed attempt to address the question of the ISCO for binary systems of comparable masses was made by Clark and Eardley [14]. They worked only to post-Newtonian order, and used an effective potential approach analogous to that used for test-body motion in the Schwarzschild geometry. Their result for r varied from $5m$ in the test-body limit (guaranteed by construction) to $2.4m$ for equal masses, in strong disagreement with the trend shown in Fig. 2. This, we believe, is a product

(i) of the restriction to post-Newtonian order, which is the first order at which an ISCO appears, and for which we found a spurious root for test bodies in Schwarzschild geometry (Table II), and (ii) of the effective potential approach, which requires an *ad hoc* switching between harmonic coordinates, in which the equations of motion are expressed, and Schwarzschild-like coordinates, in which the effective potential mimics that of the Schwarzschild geometry. It also requires repeated substitution of lower-order equations in higher-order terms, which, while formally consistent, generates uncontrolled errors in the numerical estimates. Our approach is more direct in that it finds the stable points of circular motion directly from the equations of motion, using one coordinate system consistently throughout. The only errors are those ignored in the (post)^3-Newtonian finite-mass terms, and we have tested our sensitivity to those (Fig. 6).

A quite different approach has been taken by Blackburn and Detweiler [15]. Using an initial-value formalism, they derive a variational principle for the geometry of two orbiting black holes with standing gravitational waves at spatial infinity. This leads to estimates for the effective mass and angular momentum of the system, and the angular velocity, as functions of separation. From this they can estimate the location of an ISCO, and evaluate the energy and angular momentum there. For a mass ratio of 100:1, which is essentially the test-body limit, they find values for the energy and angular momentum at the ISCO that disagree with the exact Schwarzschild values by 24% and 11%, respectively. The variational principle is not expected to estimate the separation of the ISCO accurately, and indeed their result is 60% too high. For the equal-mass case, they obtain $\tilde{E} \simeq -0.7$ and $\tilde{J} \simeq 0.85$, which are in strong disagreement with our values of $\tilde{E} \simeq -0.04$ and $\tilde{J} \simeq 3.8$. In their coordinates, the separation of the ISCO decreases by a factor of about 7 from the test-mass to the equal-mass cases, while our coordinate separation increases by 20%. Because these are different coordinate systems, such comparisons must be used with caution, but the relatively large binding energy and small angular momentum obtained by Blackburn and Detweiler suggest that they are indeed looking at black holes with separations much smaller than those indicated by our ISCO. Blackburn and Detweiler point out, however, that in the equal-mass case, the presence of gravitational radiation reaction weakens the assumption that the system is quasistatic in a rotating frame, and consequently their estimates must be regarded as merely suggestive. If our results are to be believed, they suggest that Blackburn and Detweiler have not succeeded in pinpointing the correct ISCO in the equal-mass case.

For small η, the radius of the ISCO depends roughly linearly on the mass ratio X, since $X \approx \eta$, varying from $5m$ to $5.6m$ as X varies from 0 to 0.14. The latter would correspond to a $1.4M_\odot$ neutron star coalescing onto a $10M_\odot$ black hole; the orbital frequency at the ISCO would be about 180 Hz. This variation in the ISCO radius may need to be taken into account in determining whether tidal disruption of a neutron star orbiting a massive black hole occurs before or after the unstable plunge.

For two equal-mass neutron stars of $1.4M_\odot$, the ISCO radius corresponds to a coordinate separation of about 25 km. It is useful to compare this with typical neutron-star radii, as tabulated, for example by Arnett and Bowers [16]. Converting from the radii in Schwarzschild coordinates (the usual coordinates for neutron-star models) to harmonic coordinates by subtracting $m \approx 2\,\text{km}\,(m/1.4M_\odot)$, one finds radii for $1.4M_\odot$ neutron stars ranging from 5.2 km to 8.6 km for softer equations of state (A, B, D, E, and F of [16]), from 9.8 km to 10.6 km for stiffer equations of state (C, N, and O), and 14 km for the stiffest equations of state (L and M). Thus, for all but the most stiff equations of state, the ISCO radius is greater than the sum of the nominal radii of the stars. Of course, at such separations, the tidal deformations of the stars must be taken into account. Nevertheless, these results suggest that whether tidal disruption or unstable plunge occurs first will depend sensitively on the assumed equation of state. Other authors have assumed that tidal disruption will occur first for almost equal-mass neutron star systems [12]. This question is currently under study.

In this paper, we have not discussed the effects of spin of the component bodies on the ISCO. The (post)$^{5/2}$-Newtonian equations of motion can be extended easily to include such effects as spin-orbit and spin-spin coupling (see, for example, [9]), and we have implemented such spin terms in the equations of motion as well as in the gravitational-wave forms [17]. We have studied the effects on the ISCO of spins aligned perpendicular to the orbital plane. In coalescing binary neutron stars, the effects of spin on the ISCO are expected to be small. For a $1.4M_\odot$ neutron star spinning with a period of 2 ms, the angular momentum per unit mass, which corresponds to the parameter a of the Kerr metric, may be estimated to be $0.2m$. It is unlikely that neutron stars in the late stage of coalescence will be spinning much faster than this, since, as Bildsten and Cutler [12] have argued, tidal torquing during the coalescence will be ineffective in spinning up the neutron stars to rates exceeding those they inherit from a previous mass-transfer stage. For spins of this magnitude we have shown that the effect on the ISCO is around 1%. On the other hand, if one of the bodies is a rapidly rotating Kerr black hole, the effects of rotation can be dramatic. Details of the effects of spin on the ISCO are currently being studied.

ACKNOWLEDGMENTS

We acknowledge useful discussions with Kip Thorne, Curt Cutler, and Steve Detweiler. This research was supported in part by the National Science Foundation Grant No. PHY 89-22140.

[1] C. W. Lincoln and C. M. Will, Phys. Rev. D **42**, 1123 (1990).

[2] A. G. Wiseman, Phys. Rev. D **46**, 1517 (1992).

[3] K. S. Thorne, in *300 Years of Gravitation*, edited by S. W. Hawking and W. Israel (Cambridge University Press, Cambridge, England, 1987), p. 330.

[4] A. Abramovici, W. E. Althouse, R. W. P. Drever, Y. Gürsel, S. Kawamura, F. J. Raab, D. Shoemaker, L. Sievers, R. E. Spero, K. S. Thorne, R. E. Vogt, R. Weiss, S. E. Whitcomb, and M. E. Zucker, Science **256**, 325 (1992); B. F. Schutz, Class. Quantum Grav. **6**, 1761 (1989).

[5] C. Cutler, T. A. Apostolatos, L. Bildsten, L. S. Finn, E. E. Flanagan, D. Kennefick, D. M. Markovic, A. Ori, E. Poisson, G. J. Sussman, and K. S. Thorne, Caltech Report No. GRP 316 (unpublished).

[6] C. M. Bender and S. A. Orszag, *Advanced Mathematical Methods for Scientist and Engineers* (McGraw-Hill, New York, 1978), p. 171.

[7] L. E. Kidder, C. M. Will, and A. G. Wiseman, Class. Quantum Grav. Lett. **9**, L125 (1992).

[8] T. Damour and N. Deruelle, C. R. Acad. Sci. Paris **293**, 537 (1981); **293**, 877 (1981); T. Damour, in *Gravitational Radiation*, edited by N. Deruelle and T. Piran (North-Holland, Amsterdam, 1983), p. 59; L. P. Grishchuk and S. M. Kopejkin, in *Relativity in Celestial Mechanics and Astrometry*, edited by J. Kovalevsky and V. A. Brumberg (Reidel, Dordrecht, 1986), p. 19.

[9] For a thorough review, see T. Damour, in *300 Years of Gravitation* [3], p. 128.

[10] Note that $(\text{post})^2$-Newtonian corrections to the velocities can be shown to have no effect on the transformation. Also the acceleration dependence in the two-body Lagrangian occurs only in $(\text{post})^2$-Newtonian terms, and so only the lowest-order transformation of the acceleration is needed.

[11] This simple property will not always be the case, for example, when tidal, spin-orbit, and spin-spin effects are present; these effects on the ISCO are currently under study.

[12] C. S. Kochanek, Astrophys. J. **398**, 234 (1992); L. Bildsten and C. Cutler, *ibid.* **400**, 175 (1992).

[13] *Frontiers in Numerical Relativity*, edited by C. R. Evans, L. S. Finn, and D. W. Hobill (Cambridge University Press, Cambridge, England, 1989).

[14] J. P. A. Clark and D. M. Eardley, Astrophys. J. **215**, 311 (1977).

[15] J. K. Blackburn and S. Detweiler, Phys. Rev. D **46**, 2318 (1992).

[16] D. W. Arnett and R. L. Bowers, Astrophys. J. Suppl. **33**, 415 (1977).

[17] L. E. Kidder, C. M. Will, and A. G. Wiseman, Phys. Rev. D (to be published).